

# Vessel size imaging reveals pathological changes of microvessel density and size in acute ischemia

Chao Xu<sup>1</sup>, Wolf UH Schmidt<sup>1</sup>, Kersten Villringer<sup>1</sup>, Peter Brunecker<sup>1</sup>, Valerij Kiselev<sup>2</sup>, Peter Gall<sup>2</sup> and Jochen B Fiebach<sup>1</sup>

<sup>1</sup>Center for Stroke Research Berlin (CSB), Charité-Universitätsmedizin Berlin, Berlin, Germany;

<sup>2</sup>Medical Physics, Department of Diagnostic Radiology, University Hospital Freiburg, Freiburg, Germany

**The aim of this study was to test the feasibility of vessel size imaging with precise evaluation of apparent diffusion coefficient and cerebral blood volume and to apply this novel technique in acute stroke patients within a pilot group to observe the microvascular responses in acute ischemic tissue. Microvessel density-related quantity  $Q$  and mean vessel size index ( $VSI$ ) were assessed in 9 healthy volunteers and 13 acute stroke patients with vessel occlusion within 6 hours after symptom onset. Our results in healthy volunteers matched with general anatomical observations. Given the limitation of a small patient cohort, the median  $VSI$  in the ischemic area was higher than that in the mirrored region in the contralateral hemisphere ( $P < 0.05$ ). Decreased  $Q$  was observed in the ischemic region in 2 patients, whereas no obvious changes of  $Q$  were found in the remaining 11 patients. In a patient without recanalization, the  $VSI$  hyperintensity in the subcortical area matched well with the final infarct. These data reveal that different observations of microvascular response in the acute ischemic tissue seem to emerge and vessel size imaging may provide useful information for the definition of ischemic penumbra and have an impact on future therapeutic approaches.**

*Journal of Cerebral Blood Flow & Metabolism* (2011) 31, 1687–1695; doi:10.1038/jcbfm.2011.38; published online 6 April 2011

**Keywords:** acute stroke; brain imaging; brain ischemia; MRI; perfusion-weighted MRI

## Introduction

An important focus of imaging research in the ischemic stroke is the differentiation of the ischemic penumbra from the infarct core and the normal tissue. Especially in patients presenting beyond the established time window of 4.5 hours after the stroke, in candidates for endovascular treatment, and in patients older than 80 years, a precise characterization of brain ischemia is required (Wintermark *et al*, 2008). The mismatch between ischemic areas measured by diffusion-weighted imaging (DWI) and perfusion imaging (PI) has been considered to be a good approximation of the ischemic penumbra, yet it tends to overestimate it by containing regions of benign oligemia (Heiss *et al*, 2004; Sobesky *et al*, 2005). The overestimation afflicts the clinical routine as the final infarct volume is not predicted by the

acute DWI–PI mismatch (Kidwell *et al*, 2003; Rivers *et al*, 2006). Therefore, despite its widespread use at present, the DWI–PI mismatch is not a complete approach for imaging the penumbra (Davis and Donnan, 2009; Fiebach and Schellinger, 2009; Schabitz, 2009). As the thrombolytic therapy is accompanied by a considerable risk of hemorrhage, it is necessary to develop complementary imaging modalities that can characterize the ischemic penumbra in more detail.

Cerebral microvessels, which include capillaries, small arterioles, and venules, express—together with their neighboring neurons—multiple dynamic responses to ischemia (del Zoppo and Mabuchi, 2003). The effects of ischemia on the microvasculature have so far mainly been described from the functional aspect (Ito *et al*, 2010; Zhang *et al*, 2002). Because various vasomodulators are involved in this process (Liu *et al*, 2005; Qu *et al*, 2006; Veltkamp *et al*, 2002), changes in microvascular morphology are apparently expected. Therefore, we hypothesize that the morphological variation of the microvascular network under ischemic conditions could be an effective way to describe the pathology of ischemic tissue and might provide useful information for describing the ischemic penumbra.

Considering different orders between the common clinical imaging resolution in millimeters

Correspondence: C Xu, Center for Stroke Research Berlin (CSB), Charité-Universitätsmedizin Berlin, Hindenburgdamm 30, 12200 Berlin, Germany.

E-mail: chao.xu@charite.de

This work was supported by the Federal Ministry of Education and Research via the grant Center for Stroke Research Berlin (01 EO 0801).

Received 20 October 2010; revised 31 January 2011; accepted 8 March 2011; published online 6 April 2011

and microvascular scale of micrometers, there is no way to image the microvascular network directly. Parameters reflecting properties of the local microvascular network in the imaging scale are used instead. In magnetic resonance imaging (MRI), the intravascular contrast agent increases the susceptibility difference between blood and the surrounding tissue and therefore induces the changes of the transverse relaxation rate measured by gradient echo (GE)  $\Delta R_{2GE}$  and spin echo (SE)  $\Delta R_{2SE}$ . The measurable  $\Delta R_{2GE}$  and  $\Delta R_{2SE}$  are influenced by the morphological properties of the vascular network, such as the density and diameter of the vessel population. By means of modeling and simulation, a quantity (referred to as  $Q$ ), which is the ratio of  $\Delta R_{2SE}$  and  $\Delta R_{2GE}^{2/3}$  induced by the injection of contrast agent, i.e.,  $Q = \Delta R_{2SE} / \Delta R_{2GE}^{2/3}$ , has been proposed as a measure of microvessel density (*MVD*; Jensen and Chandra, 2000). Its cubic quantity  $Q^3$  correlates significantly with histologic *MVD* (Bosomtwi *et al*, 2008; Jensen and Chandra, 2000). Kiselev *et al* (2005) further developed the model and expressed mathematically the averaged microvessel size in an imaging voxel by using a mean vessel size index (*VSI*). The *VSI* is understood as a mean vessel radius averaged over the capillary population with the weight of its volumetric fraction; therefore, it is able to monitor the dilation and contraction of microvessels. Its quantification requires accurate apparent diffusion coefficient (*ADC*), cerebral blood volume (*CBV*) and  $Q$ . By using  $Q$  and *VSI*, vessel size imaging was proposed as a novel approach to map quantitatively the cerebral microvascular structure (Tropres *et al*, 2001). This technique, which requires both SE and GE measurements, has so far two main implementations: steady-state susceptibility contrast-enhanced MRI (ssCE-MRI) and dynamic GE and SE acquisitions achieved by a special double-echo echo planar imaging (EPI) sequence. The ssCE-MRI was used in most of the studies because of its relatively low technical requirements. However, it does not record the dynamic bolus passage and only allows *VSI* qualification by additionally performing a blood test to define the contrast concentration. The later dynamic implementation was reported in a tumor study, in which the postprocessing method could be further improved (Kiselev *et al*, 2005).

Several recent studies have reported that vessel size imaging can successfully characterize cerebral tumor vascularization with elevated *MVD* and relatively stable *VSI* (Kiselev *et al*, 2005; Ungersma *et al*, 2010; Valable *et al*, 2008; Zwick *et al*, 2009). This novel technique has recently been applied to animal ischemic stroke models (Bosomtwi *et al*, 2008; Lin *et al*, 2008). Because of a much faster blood circulation in rodent models, these two studies used ssCE-MRI, which uses  $\Delta R_{2GE}$  and  $\Delta R_{2SE}$  before and after administration of an intravascular contrast agent, and thus fails to provide *CBV* evaluation and *VSI* validation. The variation in vascular density has been reported in acute (day 1) and

subacute (day 3 to 21) ischemia in rats with a focus on assessing angiogenesis. However, no data were presented in the hyperacute phase (<4.5 hours), which is especially important for clinical diagnosis.

Despite the great potential of vessel size imaging in the assessment of pathologic vascular morphology, dynamic vessel size imaging has not been so far applied in clinical stroke imaging because of its high technological requirement and extremely challenging execution of imaging acute stroke patients. Therefore, this pilot study aims to adapt the technique of vessel size imaging with dynamic SE and GE contrasts for clinical stroke application. By including the precise evaluation of *ADC* and *CBV*, the present work tests the feasibility of vessel size imaging in healthy subjects and applies this technique in patients with acute ischemic stroke to reveal the pathologic microvascular morphology in the hyperacute stage.

## Materials and methods

### Healthy Volunteers and Patients

Nine healthy volunteers (female 5; mean age 28 years, age range 25 to 40 years) were recruited in compliance with the regulations of the local ethics committee.

From October 2009 to April 2010, 15 consecutive patients with acute stroke within a time window of 4.5 hours fulfilling the criteria of having middle cerebral artery, anterior cerebral artery, or posterior cerebral artery occlusion identified by magnetic resonance angiography images were examined with the vessel size imaging protocol. In all, 13 patients had a PI-DWI mismatch and were included for further analysis. The clinical data of these 13 patients are listed in Table 1.

### Imaging

All studies were performed using a 3T clinical scanner (Tim Trio, Siemens AG, Erlangen, Germany). The *VSI* measurement was performed with a hybrid single-shot GE and SE sequence with 50 repetitions ( $TE(GE/SE)$  22/85 milliseconds; repetition time ( $TR$ ) 1,880 milliseconds; field-of-view 230 mm; slice thickness 5 mm; 16 slices; matrix size  $64 \times 64$ ). A dose of 0.13 mL Gadovist (Bayer Schering Pharma AG, Berlin, Germany) per kg body weight was injected at a speed of 5 mL/s with a time delay of 18 seconds. The *ADC* map was obtained from a six-directional DWI sequence with  $b = 1,000 \text{ s/mm}^2$  performed before the *VSI* sequence. All the measurements in stroke patients were embedded into the existing clinical imaging routine without additional time extension (Hotter *et al*, 2009).

### Data Processing

*Q* calculation: The dynamic changes in relaxation rates  $\Delta R_{2GE}$  and  $\Delta R_{2SE}$  were converted from the exponential signal drops during the bolus passage, respectively, by the

**Table 1** The clinical data in 13 acute stroke patients

ID	Age, years /sex	Time from symptom onset (hours)	Site of ischemia	NIHSS administration	NIHSS discharge	Recanalization	Acute MTT lesion volume (mL)	Acute DWI lesion volume (mL)
1	87/F	1.5	R/MCA	12	3	—	150.39	7.58
2	71/M	1.5	R/MCA	4	4	NA	57.15	4.50
3	75/M	4	R/MCA	2	1	—	44.60	0.14
4	74/M	2	R/PCA	2	1	+	30.69	0.04
5	79/F	1.5	L/MCA	18	16	NA	209.39	2.41
6	90/F	3	R/MCA	18	9	NA	199.21	50.02
7	71/M	3	R/MCA	5	4	+	77.26	0.65
8	86/F	1	L/MCA	5	0	+	53.73	4.05
9	62/M	1	R/MCA	13	0	+	96.26	2.85
10	77/F	3	R/MCA,ACA	20	20	+	79.97	54.90
11	87/F	1.5	R/MCA	6	2	+	29.57	0.01
12	89/F	1.5	L/MCA	14	13	NA	141.53	1.09
13	55/M	2	L/MCA	3	0	+	190.40	0.37
Median (IQR)	77 (71–87)	1.5 (1.5–3)	—	6 (4–14)	3 (1–9)	—	79.97 (53.73–150.39)	2.41 (0.37–4.5)

DWI, diffusion-weighted imaging; F, female; IQR, interquartile range; L, left; M, male; MCA, middle cerebral artery; MTT, mean transit time; NA, no follow-up examination was available; NIHSS, National Institutes of Health Stroke Scale; R, right; +, recanalization happened in the follow-up examination; —, no recanalization.

following equation:

$$\Delta R_2(t) = -\frac{1}{TE} \log\left(\frac{S(t)}{S_0}\right), \quad (1)$$

where  $TE$  is the echo time,  $S_0$  is the average baseline signal and  $S(t)$  is the signal density along the timeline. Given that

$$Q \equiv \Delta R_{2SE} / \Delta R_{2GE}^{2/3}, \quad (2)$$

$Q$  was obtained by fitting the linear dependence between  $\Delta R_{2SE}(t)$  and  $\Delta R_{2GE}(t)^{2/3}$  by using the least-square procedure.

**Vessel size index calculation:** The  $VSI$  map was calculated by the equation (Kiselev *et al*, 2005):

$$VSI = 0.867 \times (ADC \times CBV)^{1/2} / Q^{3/2} \quad (3)$$

$ADC$  maps from the diffusion measurement were coregistered to the baseline SE images by using SPM8 (Wellcome Department of Imaging Neuroscience, University College London, London, UK). The dynamic  $\Delta R_{2GE}(t)$ , which is proportional to tracer concentration  $C_t(t)$ , i.e.,  $C_t(t) \propto \Delta R_{2GE}(t)$ , was used to calculate the  $CBV$  map (Ostergaard *et al*, 1996). Cerebral blood volume can be determined from area under the tissue impulse response curve  $R(t)$ :

$$CBV = \int_0^\infty R(t) \cdot dt \quad (4)$$

It is well known in perfusion theory that tracer-concentration curve  $C_t(t)$  is the tissue response to the arterial input function:

$$C_t(t) = CBF \times C_a(t) \otimes R(t), \quad (5)$$

where  $CBF$  is cerebral blood flow,  $\otimes$  indicates convolution, and  $C_a(t)$  is the arterial input function.

In this study, arterial input function was selected manually in the M3 segment at the top of the ventricle contralateral to the suspected ischemia to yield a relatively high signal-to-noise ratio ( $SNR$ ; Ebinger *et al*, 2010). The deconvolution of  $R(t)$  from equation (5) was accomplished in Fourier domain by applying the Tikhonov regularization

with a control parameter optimized according to the voxel-wise baseline  $SNR$  as  $\lambda = 10^{3.7/SNR^{2.7}}$  by the following equation:

$$R(\omega) = \frac{1}{CBF} \times \frac{C_t(\omega)C_a^*(\omega)}{C_a(\omega)C_a^*(\omega) + \lambda^2\omega^4} \quad (6)$$

where  $R(\omega)$ ,  $C_t(\omega)$ , and  $C_a(\omega)$  are the transformation of  $R(t)$ ,  $C_t(t)$ , and  $C_a(t)$  in Fourier domain, respectively, and  $C_a^*(\omega)$  is the conjugate of  $C_a(\omega)$  (Gall *et al*, 2010). Finally,  $CBV$  was normalized to a global average in the healthy tissue of 3% (Ostergaard *et al*, 1999) and used in equation (3) to derive  $VSI$ .

### Regions of interest Selection

For each healthy volunteer, the regions of interest (ROIs) of gray matter (GM) and white matter (WM) were generated from probability maps by using the segmentation method in SPM8, with the probability value being higher than 0.5. The ROIs of thalamus were manually drawn on pre-processed SE images. For each stroke patient, DWI lesion was manually delineated by a human rater masked to other images. The derived ROI was then mapped to  $ADC$  images to ensure  $ADC$  hypointensities ( $ADC < 0.7 \mu\text{m}^2/\text{milli-seconds}$ ) and exclude the false-positive region automatically. Mean transit time (MTT)  $> 5.3$  seconds was set to be the initial threshold for hypoperfused tissue (Zaro-Weber *et al*, 2010). The selected MTT ROI was corrected manually to exclude areas that were not part of a credible perfusion deficit. An example from patient 8 is shown to illustrate the procedures to generate ROIs in Figure 1. All the ROIs and postprocessed maps were normalized to the standard space to derive two spatially symmetric hemispheres. The ROI of the ischemic tissue, i.e., tissue at risk, was defined as the subtracted region MTT minus DWI ROI. The ischemic ROI was then mirrored to the contralateral region with normal tissue. The ischemic and mirrored ROI were superimposed on normalized  $Q$  and  $VSI$  maps for evaluation.

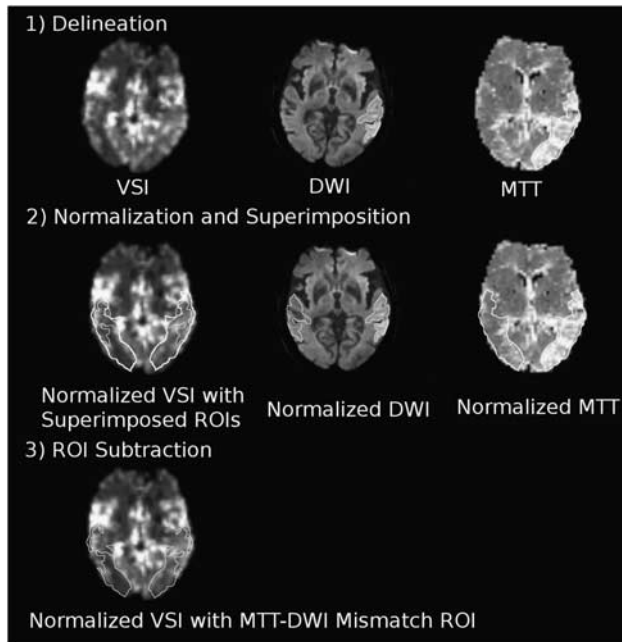


**Figure 1** Procedures to generate the ischemic and mirrored regions of interests (ROIs). Images are taken from patient 8. (1) Diffusion-weighted imaging (DWI) and mean transit time (MTT) ROIs are delineated while masked to other images. (2) DWI, MTT, and vessel size index (VSI) maps, as well as ROIs derived from step 1, are normalized to the standard brain with two spatially symmetric hemispheres. Normalized DWI and MTT ROIs are mirrored to the contralateral hemisphere. Both pairs of symmetric ROIs were superimposed on normalized VSI maps. (3) The area corresponding to MTT ROI minus DWI ROI is defined as the ischemic tissue. Its mirrored ROI is placed in the contralateral hemisphere with normal tissue.

## Statistical Analyses

Shapiro–Wilk test confirmed that  $Q$  and  $VSI$  in both ischemic ROI and contralateral mirrored ROI did not follow the normal distribution. Therefore, median and full-width at half-maximum (FWHM), rather than mean value and standard deviation, were used to characterize the voxel distribution in each patient, as well as in healthy subjects. The median and FWHM of  $VSI$  and  $Q$  in patients between ROIs were tested by Wilcoxon's signed-rank test ( $n = 13$ ).

## Results

The histogram of voxel-wise  $Q$  and  $VSI$  values gathered from nine healthy subjects in three selected ROIs of GM, WM, and thalamus are shown in Figure 2.  $Q$  is higher in GM and thalamus than in WM, i.e., higher MVD is observed in GM and thalamus than in WM, according to the linear dependency of  $MVD$  and  $Q^3$ . Similar vessel sizes are observed in GM (median,  $13.8 \mu\text{m}$ ; FWHM,  $12.4 \mu\text{m}$ ) and WM (median,  $13.1 \mu\text{m}$ ; FWHM,  $10.7 \mu\text{m}$ ). In the thalamus with the absence of large vessels, smaller  $VSI$  (median,  $9.1 \mu\text{m}$ ; FWHM,  $8.1 \mu\text{m}$ ) is found.

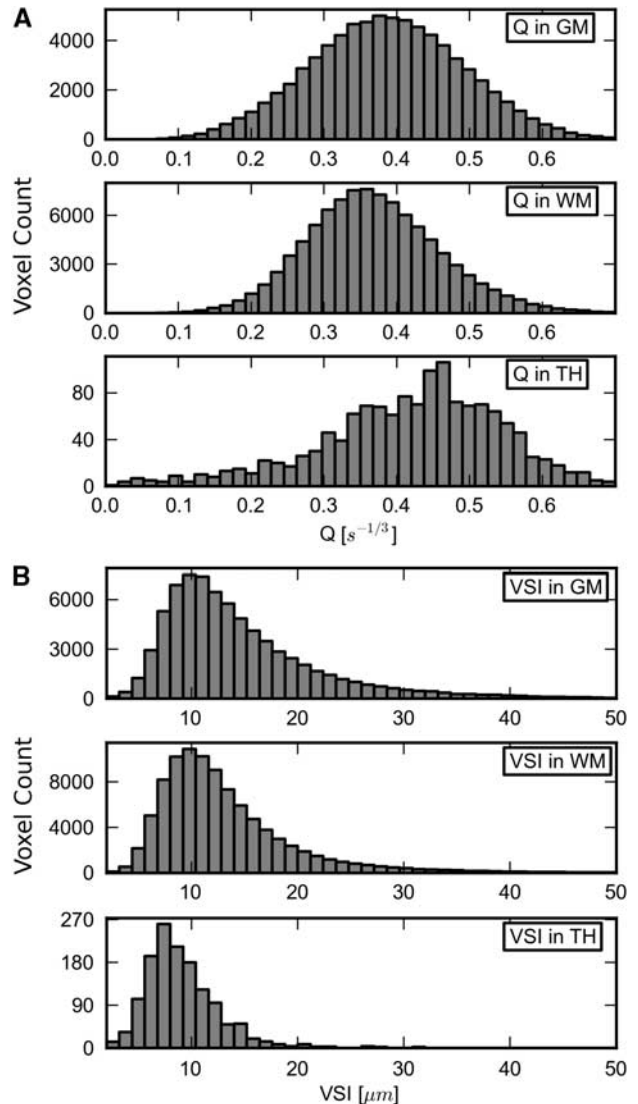


**Figure 2** Histograms of (A)  $Q$  and (B) vessel size index ( $VSI$ ) values in voxels gathered from nine healthy subjects in the regions of interest of gray matter (GM), white matter (WM), and thalamus (TH).

Figure 3 illustrates the median and FWHM of  $Q$  and  $VSI$  distribution in each patient in the ischemic area and its mirrored ROI in the contralateral hemisphere. Elevated median  $VSI$  value has been detected in the ischemic tissue compared with the contralateral region ( $n = 13$ ,  $P < 0.05$ ). Changes in the median of  $Q$  between ischemic and mirrored ROI are rather heterogeneous. Predominantly reduced median  $Q$  (the change of value from ischemic ROI to mirrored ROI  $> 10\%$ ) in the ischemic region is found in 2 of 13 patients, whereas median  $Q$  in the remaining 11 patients does not show an obvious change. The FWHM of the distribution in ischemic tissue is increased in  $VSI$  ( $n = 13$ ,  $P < 0.05$ ) and decreased in  $Q$  ( $n = 13$ ,  $P < 0.05$ ).

Different pathological responses of the microvascular structure to the ischemia seem to emerge. In 11 of the 13 patients (patients 1 to 11), with a typical example shown in Figure 4, the  $Q$  map appears rather homogeneous, whereas

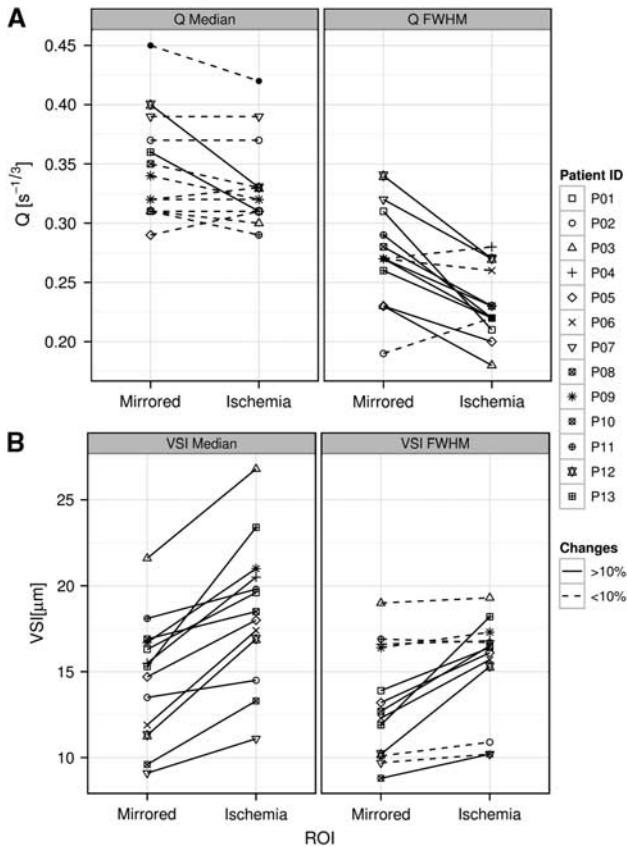


**Figure 3** Trend plots of median and full-width at half-maximum (FWHM) in (A)  $Q$  and (B) vessel size index ( $VSI$ ) in 13 patients. Data points are labeled by the patient ID corresponding to Table 1. Different line styles are used to identify the percentage change of value in the ischemic regions of interest (ROI) compared with the mirrored ROI. The change of value from the ischemic ROI to the mirrored ROI in percentage that is higher than 10% is presented by a solid line, and the change of lower than 10% is labeled by a dash line.

the hyperintensities on the  $VSI$  map are observed in the perfusion deficit. Consistent with the maps, the shape of the  $Q$ -value histogram in the hypoperfused region displays no obvious changes compared with the mirrored area, whereas the peak of the  $VSI$  histogram in the ischemia shifts toward larger values. In the remaining two patients (patients 12 and 13), hypointensities on the  $Q$  map and hyperintensities on the  $VSI$  map are shown in the perfusion lesion (see the example in Figure 5). The  $Q$  histogram in the ischemic region shifts toward smaller values, whereas the  $VSI$  histogram becomes broader and moves toward larger values.

Follow-up result of magnetic resonance angiography was available for 8 of the 13 patients and showed recanalization in 6 patients. In the subgroup of patients without recanalization (patients 1 and 3), the  $VSI$  map in the hyperacute stage was compared with the fluid attenuation inversion recovery image on day 6 identifying the final infarct size. Increased  $VSI$  and decreased  $Q$  values in the subcortical area (arrowed in Figure 6) matched well with the final infarct core.

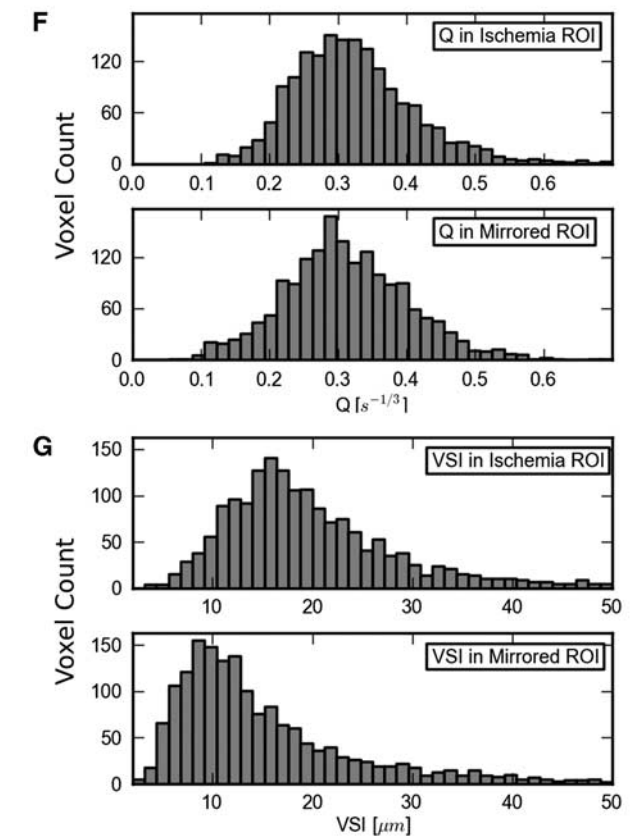
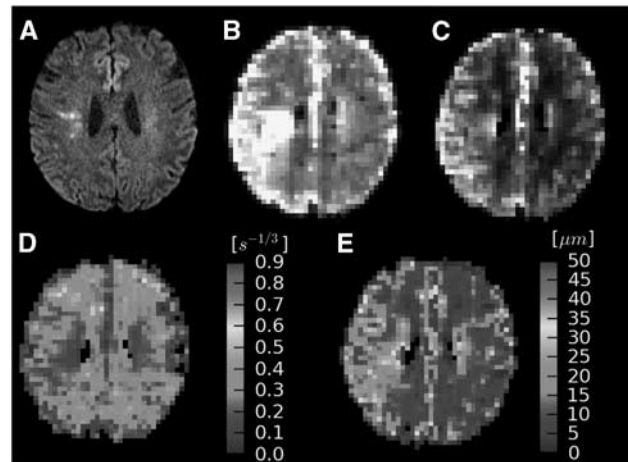


**Figure 4** Images from patient 9 and histograms of  $Q$  and vessel size index ( $VSI$ ) in ischemia and its mirrored regions of interest (ROI). Images in acute phase: (A) diffusion-weighted imaging, (B) mean transit time, (C) cerebral blood volume, (D)  $Q$ , and (E)  $VSI$ . Histograms of voxel-wise (F)  $Q$  and (G)  $VSI$  in the ischemic region (top) and its mirrored ROI in the contralateral hemisphere (bottom).

## Discussion

### Feasibility of Vessel Size Imaging in Acute Stroke

Although the theoretical concept of vessel size imaging has been studied since 1998 (Dennie *et al*, 1998; Tropres *et al*, 2001), the execution has been

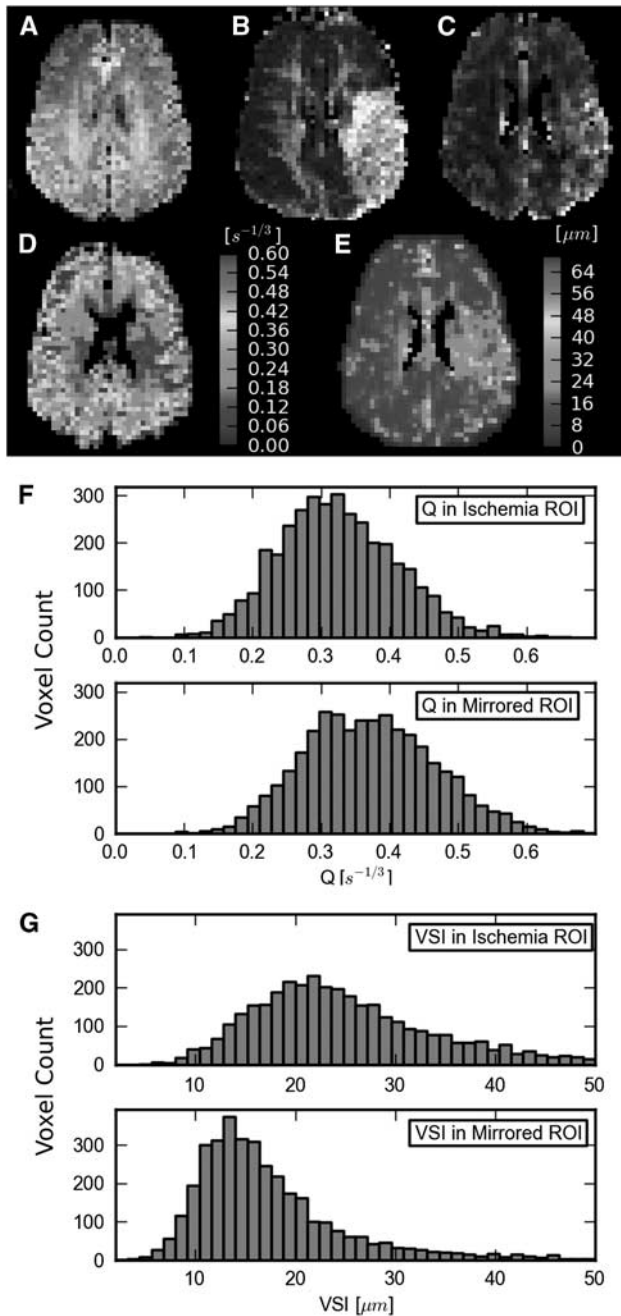


**Figure 5** Images from patient 13 and histograms of  $Q$  and vessel size index ( $VSI$ ) in ischemia and its mirrored regions of interest (ROI). Images in acute phase: (A) diffusion-weighted imaging, (B) mean transit time, (C) cerebral blood volume, (D)  $Q$ , and (E)  $VSI$ . Histograms of voxel-wise (F)  $Q$  and (G)  $VSI$  in the ischemic region (top) and its mirrored ROI in the contralateral hemisphere (bottom).

complicated by the acquisition of both GE and SE contrasts in a single repetition time during the dynamic bolus passage. The ssCE-MRI that uses GE and SE measurements before and after administration of an intravascular contrast agent is a compromised technique to obtain  $\Delta R_{2GE}$  and  $\Delta R_{2SE}$  in the steady state and is so far used in most of the tumor

and experimental stroke studies. However, this method is not suitable for clinical acute stroke imaging because of time constraints and the high dose of contrast agent required to reach a measurable steady state. It produces  $VSI$  quantification by performing an additional blood test, as  $CBV$  cannot be assessed without dynamic imaging. Our pilot study has successfully accomplished dynamic GE and SE measurements in acute stroke patients by using a double-echo EPI sequence. The GE acquisition substitutes the standard PI measurement, which is part of the clinical imaging protocol. Therefore, vessel size imaging can be embedded in routine measurements without any time extension. However, this technique limits the time for read-out gradients and thus restricts the image matrix to  $64 \times 64$ , which is only half of the resolution of single-echo perfusion images. Although parallel acquisition may overcome this limitation, it will reduce the image quantity to a great extent (Griswold *et al*, 2002). To maintain the spatial resolution, some studies performed separate conventional GE and SE acquisitions with dual injection of contrast agent to enable vessel size imaging (Hsu *et al*, 2009). Although the dual injection method avoids the sacrifice of image resolution, it brings other problems into discussion: the possible influence of the residual contrast agent from the first injection on the second one, the potential temporal misregistration between two time series and the increased total dose of the contrast agent. Furthermore, the prolonged measurement time of dual injection does not meet the crucial time limit of acute stroke imaging. The duo-echo technique used in this study with a voxel size of  $3.6 \times 3.6 \times 5 \text{ mm}^3$  is appropriate for acute stroke patients and provides MTT maps with diagnostic value (see MTT map on Figures 1, 4, 5 and 6).

Estimating  $MVD$  from  $Q$  according to the linear correlation  $MVD = k \times Q^3$  requires the assessment of the correlation efficient  $k$  (Jensen and Chandra, 2000). In the mouse brain,  $k$  has been proposed as  $329 \text{ s/mm}^2$  by Wu *et al* (2004), yet it is not available for the human brain. Jensen *et al* (2006) showed a possible way to calculate the lower and upper bounds of  $MVD$  *in vivo* by using  $Q$ . However, the lower and upper boundaries, which differ by two orders of magnitude, do not allow an accurate estimate of  $MVD$ . Therefore, we use  $Q$  as the parameter, indicating the relative change of  $MVD$  instead of the quantitative  $MVD$ .

One study has published a quantitative  $Q$  assessment in human brain tissue (Jensen *et al*, 2006). The  $Q$  values in our study are somewhat lower than those found by Jensen *et al*, in which a triple dose of contrast agent has been administered and only the maximum signal drop points are used to estimate  $Q$ . Although such an implementation leads to a smaller underestimation of  $Q$  in the circumstance of intrinsic paramagnetism, it is not suitable for acute stroke imaging: first, such a high dose of contrast agent is not commonly used in clinical routine;

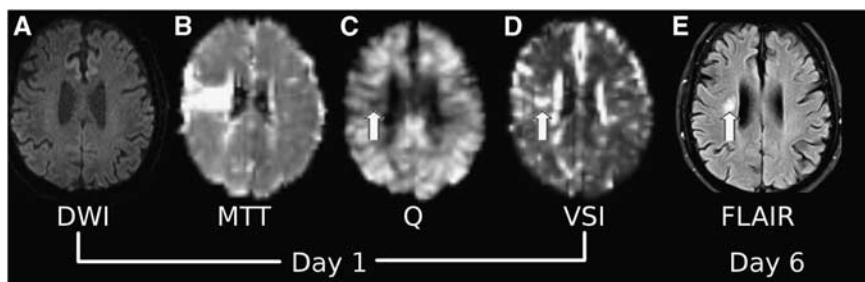


**Figure 6** Images from patient 3 on day 1 and day 6. (A) Diffusion-weighted imaging (DWI), (B) mean transit time (MTT), (D) vessel size index (VSI) on day 1, and (E) fluid attenuation inversion recovery (FLAIR) on day 6. The hypointensity on (C) Q and hyperintensity on VSI matches the final infarction on FLAIR (pointed by the arrow).

second, maximum signal drops between ischemic and normal tissue are not comparable, as the maximum drop in ischemic tissue is reached much later than in normal tissue with a significantly lower concentration of contrast agent. Therefore, we have fitted the whole dynamic passage for the estimation of  $Q$  to achieve a relatively equivalent influence of contrast agent dosage in both the ischemic and the normal tissue. Moreover, linear fitting avoids the accidental errors that often occur in picking a single signal drop.

The method in this study is based on the tissue model introduced by Kiselev *et al* (2005), which results in a systematic overestimation of vessel sizes. The VSI we measured in the thalamus, where no large vessels present, is very similar to the value of  $7.2\ \mu\text{m}$  proposed by the microscale tissue model (Kiselev *et al*, 2005). Jochimsen *et al* (2010) assessed venous VSI in healthy human brains with the administration of carbogen by measuring the induced blood oxygenation level-dependent effect in a 7T scanner. Despite the different techniques, the vessel radii of GM and WM in our healthy volunteers are very similar to their venous vessel radii. The vessel sizes of the normal-appearing tissue in tumor patients studied by Hsu *et al* (2009) and Kiselev *et al* (2005) are almost twice as large as our results in healthy brain tissue. Besides the possible vascular compensation in the normal-appearing tissue around the tumor, the difference in results is mainly because we normalized the global CBV to 3%, which has been found to be a better estimation to the real blood volume fraction than the 6% used by their groups. Moreover, considering that the VSI quantification depends on the assessment of CBV, the deconvolution with SNR-adapted regularization applied in our study allows an accurate estimation of CBV, which is more advanced than the integration of dynamic bolus passage or the fitting of the gamma function in previous studies.

The variation of MVD and VSI among three cerebral regions found in the healthy volunteers matched very well with general anatomical observations (Cavaglia *et al*, 2001), i.e., the diameter of microvessels in WM and GM is very similar and lower vessel density is observed in WM than in GM.

It indicates that vessel size imaging is a reliable and feasible technique to assess the microvascular morphology *in vivo*.

### Standard Perfusion Parameters and Vessel Size Imaging

Vessel size imaging uses both dynamic GE and SE contrasts, whereas standard PI uses GE only. It is well known that GE contrast is sensitive to vessels of all sizes and SE contrast is weighted toward microvascular structure (Zhao *et al*, 2006). Therefore, VSI provides an insight into the properties of microvasculature, which are often shielded in GE perfusion measurement predominated by large vessels. Considering that VSI is a quantitative parameter, it enables a comparison in inter-subject and longitudinal studies. This is an obvious advantage compared with perfusion parameters such as CBV and CBF presenting as relative values and MTT influenced heavily by the injecting condition of contrast agent. However, one has to keep in mind that the change of VSI is inevitably dependent on the variation of CBV. When the MVD remains unchanged, the VSI map has a similar appearance to the relative CBV contrast.

### Ischemic Penumbra and Vessel Size Imaging

Figure 6 illustrates the interesting match between the predominant changes in acute VSI and  $Q$  maps and the final infarction in patient 3. It may indicate that severe damage of microvasculature obstructs the reperfusion and leads to tissue infarction. However, the possible correlation of increased VSI and decreased  $Q$  to the development of irreversible infarct cannot be confirmed. But, the lesions visible in the  $Q$  and VSI maps are always confined within the territory of MTT hyperintensities. Typically, in Figure 5, the hyperintensity on the VSI map only partially matches the MTT lesion, displaying a mismatch at the posterior part. Given the fact of the overestimation of the perfusion map, VSI might provide a better estimate of the ischemic penumbra from the aspect of microvascular structure.

## Microvascular Response to Ischemia in the Hyperacute Phase

Given the limitation of a few patients, increased *VSI* in the ischemic region agrees with the observation from relative measurements of vessel size in rats. Reduced *Q* values in patients 12 and 13 fit to the decreased *Q* in the ischemic tissue in rats after transient focal ischemia (Lin *et al*, 2008). The values of *Q* and *VSI* vary among patients owing to different territories being involved in ischemia for each patient. The varied FWHM of *Q* and *VSI* distribution reveals that the changes may be regionally heterogeneous.

According to the observation in a pilot group of patients, we suggest that our data support the serial responses in the microvascular network to ischemia during the cerebral hemodynamic compromise (Powers, 1991). As cerebral perfusion pressure falls after the occlusion, precapillary resistance vessels dilate to maintain *CBF*, which may account for our observation of increased vessel sizes. One should notice that the change of *VSI* is relatively small (at most 50% in our observation), which could be explained by the limited extent to which blood vessels can dilate. Once maximum vasodilatation has been reached, autoregulation fails and progressive increases in cerebral oxygen extraction can temporarily maintain cerebral oxygen metabolism. As perfusion pressure continues to fall, a disruption of cellular metabolism and microvascular obstruction occur (Ito *et al*, 2010), which is likely the cause of the decreased *MVD* within the ischemic region in patients 12 and 13. Moreover, the edema results in a more pronounced compression of small capillaries as compared with arterioles and venules, leading to a shift in the calculated average vessel size to larger values. However, no successive studies are currently available to monitor the extending microvascular changes after ischemic injury and the associated longitudinal vascular responses are not comparable between individual patients.

To sum up, our pilot results show that vessel size imaging is feasible in stroke patients. Further research is required to better understand microvascular response in the acute ischemic tissue. Longitudinal MR examinations might help to correlate vessel size imaging to tissue fate and thus improve treatment tailoring.

## Disclosure/conflict of interest

The authors declare no conflict of interest.

## References

Bosomtvi A, Jiang Q, Ding GL, Zhang L, Zhang ZG, Lu M, Ewing JR, Chopp M (2008) Quantitative evaluation of microvascular density after stroke in rats using MRI. *J Cereb Blood Flow Metab* 28:1978–87

- Cavaglia M, Dombrowski SM, Drazba J, Vasanji A, Bokesch PM, Janigro D (2001) Regional variation in brain capillary density and vascular response to ischemia. *Brain Res* 910:81–93
- Davis SM, Donnan GA (2009) MR mismatch and thrombolysis: appealing but validation required. *Stroke* 40:2910
- del Zoppo GJ, Mabuchi T (2003) Cerebral microvessel responses to focal ischemia. *J Cereb Blood Flow Metab* 23:879–94
- Dennie J, Mandeville JB, Boxerman JL, Packard SD, Rosen BR, Weisskoff RM (1998) NMR imaging of changes in vascular morphology due to tumor angiogenesis. *Magn Reson Med* 40:793–9
- Ebinger M, Brunecker P, Jungehulsing GJ, Malzahn U, Kunze C, Endres M, Fiebach JB (2010) Reliable perfusion maps in stroke MRI using arterial input functions derived from distal middle cerebral artery branches. *Stroke* 41:95–101
- Fiebach JB, Schellinger PD (2009) MR mismatch is useful for patient selection for thrombolysis: yes. *Stroke* 40:2906–7
- Gall P, Emerich P, Kjølby B, Kellner E, Mader I, Kiselev V (2010) On the design of filters for fourier and oSVD-based deconvolution in bolus tracking perfusion MRI. *Magn Reson Mater Phy* 23:187–95
- Griswold MA, Jakob PM, Heidemann RM, Nittka M, Jellus V, Wang J, Kiefer B, Haase A (2002) Generalized autocalibrating partially parallel acquisitions (GRAPPA). *Magn Reson Med* 47:1202–10
- Heiss W-D, Sobesky J, Smekal Uv, Kracht LW, Lehnhardt F-G, Thiel A, Jacobs AH, Lackner K (2004) Probability of cortical infarction predicted by flumazenil binding and diffusion-weighted imaging signal intensity: a comparative positron emission tomography/magnetic resonance imaging study in early ischemic stroke. *Stroke* 35:1892–8
- Hotter B, Pittl S, Ebinger M, Oepen G, Jegzentis K, Kudo K, Rozanski M, Schmidt W, Brunecker P, Xu C, Martus P, Endres M, Jungehulsing G, Villringer A, Fiebach J (2009) Prospective study on the mismatch concept in acute stroke patients within the first 24 hours after symptom onset—1000Plus study. *BMC Neurol* 9:60
- Hsu Y-Y, Yang W-S, Lim K-E, Liu H-L (2009) Vessel size imaging using dual contrast agent injections. *J Magn Reson Imaging* 30:1078–84
- Ito U, Hakamata Y, Kawakami E, Oyanagi K (2010) Temporary focal cerebral ischemia results in swollen astrocytic endfeet that compress microvessels and lead to focal cortical infarction. *J Cereb Blood Flow Metab* 31:328–38
- Jensen JH, Chandra R (2000) MR imaging of microvasculature. *Magn Reson Med* 44:224–30
- Jensen JH, Lu H, Inglese M (2006) Microvessel density estimation in the human brain by means of dynamic contrast-enhanced echo-planar imaging. *Magn Reson Med* 56:1145–50
- Jochimsen TH, Ivanov D, Ott DVM, Heinke W, Turner R, Möller HE, Reichenbach JR (2010) Whole-brain mapping of venous vessel size in humans using the hypercapnia-induced BOLD effect. *Neuroimage* 51:765–74
- Kidwell CS, Alger JR, Saver JL (2003) Beyond mismatch: evolving paradigms in imaging the ischemic penumbra with multimodal magnetic resonance imaging. *Stroke* 34:2729–35
- Kiselev VG, Strecker R, Ziyeh S, Speck O, Hennig J (2005) Vessel size imaging in humans. *Magn Reson Med* 53:553–63

- Lin C-Y, Chang C, Cheung W-M, Lin M-H, Chen J-J, Hsu CY, Chen J-H, Lin T-N (2008) Dynamic changes in vascular permeability, cerebral blood volume, vascular density, and size after transient focal cerebral ischemia in rats: evaluation with contrast-enhanced magnetic resonance imaging. *J Cereb Blood Flow Metab* 28:1491–501
- Liu D, Wu L, Breyer R, Mattson MP, Andreasson K (2005) Neuroprotection by the PGE2 EP2 receptor in permanent focal cerebral ischemia. *Ann Neurol* 57:758–61
- Ostergaard L, Chesler DA, Weisskoff RM, Sorensen AG, Rosen BR (1999) Modeling cerebral blood flow and flow heterogeneity from magnetic resonance residue data. *J Cereb Blood Flow Metab* 19:690–9
- Ostergaard L, Weisskoff RM, Chesler DA, Gyldensted C, Rosen BR (1996) High resolution measurement of cerebral blood flow using intravascular tracer bolus passages. Part I: mathematical approach and statistical analysis. *Magn Reson Med* 36:715–25
- Powers WJ (1991) Cerebral hemodynamics in ischemic cerebrovascular disease. *Ann Neurol* 29:231–40
- Qu K, Chen CP, Halliwell B, Moore PK, Wong PT (2006) Hydrogen sulfide is a mediator of cerebral ischemic damage. *Stroke* 37:889–93
- Rivers CS, Wardlaw JM, Armitage PA, Bastin ME, Carpenter TK, Cvorovic V, Hand PJ, Dennis MS (2006) Do acute diffusion- and perfusion-weighted MRI lesions identify final infarct volume in ischemic stroke? *Stroke* 37:98–104
- Schabitz W-R (2009) MR mismatch is useful for patient selection for thrombolysis: no. *Stroke* 40:2908–9
- Sobesky J, Weber OZ, Lehnhardt F-G, Hesselmann V, Neveling M, Jacobs A, Heiss W-D (2005) Does the mismatch match the penumbra?: magnetic resonance imaging and positron emission tomography in early ischemic stroke. *Stroke* 36:980–5
- Tropres I, Grimault S, Vaeth A, Grillon E, Julien C, Payen J-F, Lamalle L, Décorps M (2001) Vessel size imaging. *Magn Reson Med* 45:397–408
- Ungersma SE, Pacheco G, Ho C, Yee SF, Ross J, Bruggen N, Peale FV, Jr, Ross S, Carano RAD (2010) Vessel imaging with viable tumor analysis for quantification of tumor angiogenesis. *Magn Reson Med* 63:1637–47
- Valable S, Lemasson B, Farion R, Beaumont M, Segebarth C, Remy C, Barbier EL (2008) Assessment of blood volume, vessel size, and the expression of angiogenic factors in two rat glioma models: a longitudinal *in vivo* and *ex vivo* study. *NMR Biomed* 21:1043–56
- Veltkamp R, Rajapakse N, Robins G, Puskar M, Shimizu K, Busija D (2002) Transient focal ischemia increases endothelial nitric oxide synthase in cerebral blood vessels. *Stroke* 33:2704–10
- Wintermark M, Albers GW, Alexandrov AV, Alger JR, Bammer R, Baron J-C, Davis S, Demaerschalk BM, Derdeyn CP, Donnan GA, Eastwood JD, Fiebach JB, Fisher M, Furie KL, Goldmakher GV, Hacke W, Kidwell CS, Kloska SP, Kohrmann M, Koroshetz W, Lee T-Y, Lees KR, Lev MH, Liebeskind DS, Ostergaard L, Powers WJ, Provenzale J, Schellinger P, Silbergleit R, Sorensen AG, Wardlaw J, Wu O, Warach S (2008) Acute stroke imaging research roadmap. *Stroke* 39:1621–8
- Wu EX, Tang H, Jensen JH (2004) High-resolution MR imaging of mouse brain microvasculature using the relaxation rate shift index Q. *NMR Biomed* 17:507–12
- Zaro-Weber O, Moeller-Hartmann W, Heiss WD, Sobesky J (2010) MRI perfusion maps in acute stroke validated with 15O-water positron emission tomography. *Stroke* 41:443–9
- Zhang ZG, Zhang L, Tsang W, Soltanian-Zadeh H, Morris D, Zhang R, Goussev A, Powers C, Yeich T, Chopp M (2002) Correlation of VEGF and angiopoietin expression with disruption of blood-brain barrier and angiogenesis after focal cerebral ischemia. *J Cereb Blood Flow Metab* 22:379–92
- Zhao F, Wang P, Hendrich K, Ugurbil K, Kim SG (2006) Cortical layer-dependent BOLD and CBV responses measured by spin-echo and gradient-echo fMRI: insights into hemodynamic regulation. *Neuroimage* 30:1149–60
- Zwick S, Strecker R, Kiselev V, Gall P, Huppert J, Palmowski M, Lederle W, Woenne EC, Hengerer A, Taupitz M, Semmler W, Kiessling F (2009) Assessment of vascular remodeling under antiangiogenic therapy using DCE-MRI and vessel size imaging. *J Magn Reson Imaging* 29:1125–33